

## Chapter III: Experimental

This chapter describes the methodology to synthesise the nanoparticles and nanowires; deposit thin films and the experimental techniques used to characterise them. Synthesis of  $Ti_{1-x}Co_xO_2$  nanoparticles/nanowires as well as thin film deposition techniques used in the present work are given in Section 3.1. A brief description about the ion irradiation technique is appended in Section 3.2. In Section 3.3, various characterisation techniques used in the present work are discussed.

### 3.1 Synthesis/Deposition Techniques

In this section, sol-gel and hydrothermal techniques used to synthesise  $Ti_{1-x}Co_xO_2$  nanoparticles are discussed. The e-beam evaporation and pulsed laser deposition (PLD) techniques used in the present study for the film deposition are briefly outlined.

#### 3.1.1 Synthesis of Nanoparticles by Sol-Gel Technique

$TiO_2$  nanoparticles were synthesised using analytical grade titanium butoxide ( $Ti(OC_4H_9)_4$ ; Sigma Aldrich) as a precursor and methoxyethanol ( $C_3H_8O_2$ ; MERCK) as a solvent. Few drops of  $HNO_3$  (MERCK) were added slowly to the solution as a stabilizer. By adjusting the volume ratio of titanium butoxide and methoxyethanol in the range of 1:25 and 1:7, the  $pH$  level was changed from 4.5 to 6.5, respectively measured using a digital  $pH$  meter. Water was added to initiate the hydrolysis process. The precipitate was filtered and dried at  $100\text{ }^\circ\text{C}$ . The final products were calcined at 300, 500, 650, 800 and  $850\text{ }^\circ\text{C}$ . The experimental scheme for synthesis of  $TiO_2$  nanoparticles is illustrated in Fig.3.1. For Co-doped  $TiO_2$  nanoparticles, cobalt acetate ( $Co(CH_3CO_2)_2$ ; HIMEDIA) solution was added to the titanium butoxide and methoxyethanol solution and was stirred for 1h for uniform mixing before hydrolysis. The  $pH$  was maintained at 6.5. Concentration of Co was calculated for 1, 3 and 5 at.% with respect to  $TiO_2$ . The hydrolyzed samples were filtered, washed, dried and calcined at  $500\text{ }^\circ\text{C}$  to obtain the final products. Detailed scheme of synthesis is shown in Fig. 3.2.

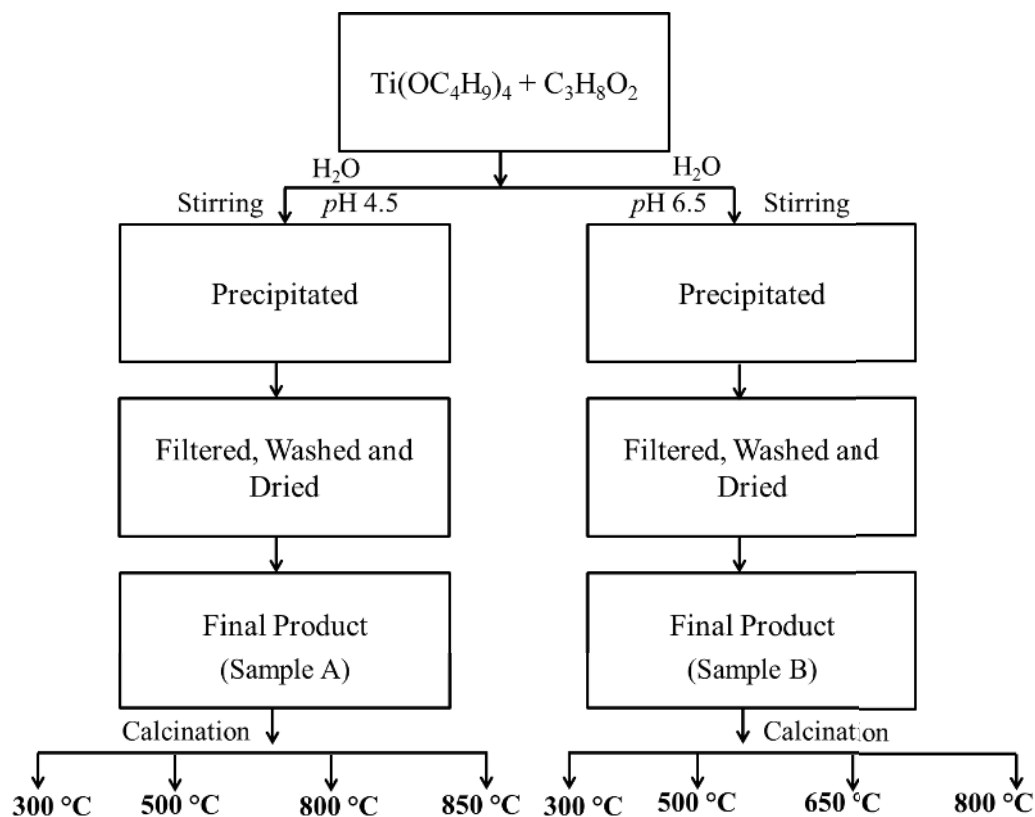


**Fig.3.1** Experimental scheme for synthesis of TiO<sub>2</sub> nanoparticles.

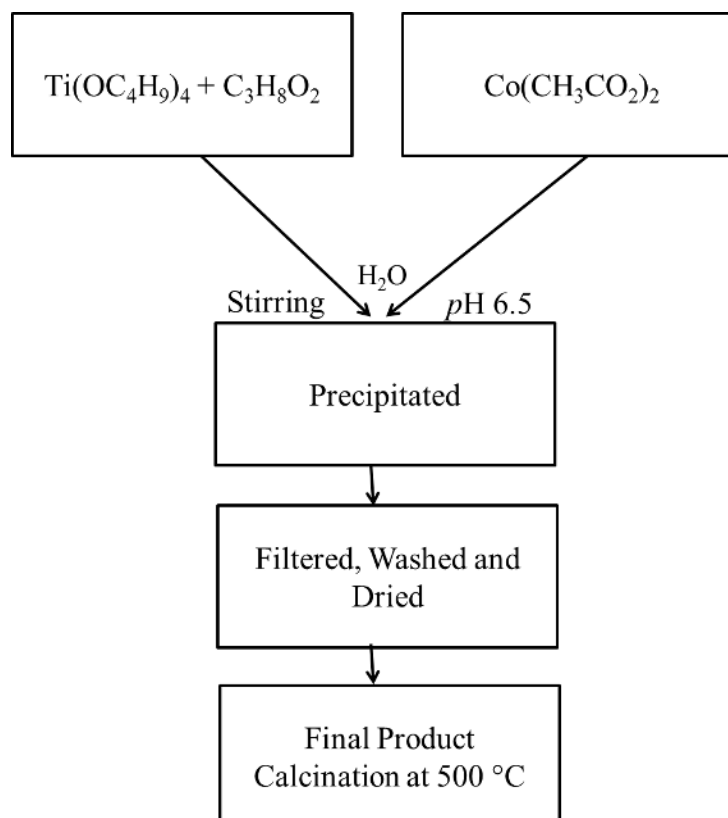


**Fig.3.2** Experimental scheme for synthesis of Co-doped TiO<sub>2</sub> nanoparticles.

### 3.1.2 Synthesis of Nanowires by Hydrothermal Technique

Hydrothermal processing is an innovative tool to synthesise the particles in different morphologies in presence of high pressure and temperature. It also enables uniform distribution of particles. The reactor has provisions for gas inlet/outlet, sampling and internal cooling. A magnetic drive is attached to the head for stirring purpose. For mixing, bladed impellers are attached with the shaft. A Teflon liner is provided to be kept inside the stainless steel container to



**Fig.3.3** Parr autoclave (450 ml: Model 4560, USA) used for the hydrothermal reaction.

insulate the sample from the wall. Temperature is controlled through a PID control with a digital display showing temperature, pressure and rotor speed. Pressure of the reactor unit is measured with a transducer attachment. In a conventional experiment, desired amount of materials were poured into the reactor and the reactor head was fitted over the bomb and tightened. A thermocouple was inserted into the thermo valve followed by switching on the heater. Specific temperature and desired rotational speed were achieved by proper adjustment of controllers provided for the purpose. The autogenous pressure and temperature was shown on the display. A typical photograph of the autoclave used is shown in Fig.3.3 2g of TiO<sub>2</sub> nanoparticles (sample A<sub>1</sub>)

synthesised through hydrothermal technique were used for the growth of nanowires as schematically shown in the flowchart (Fig.3.4).

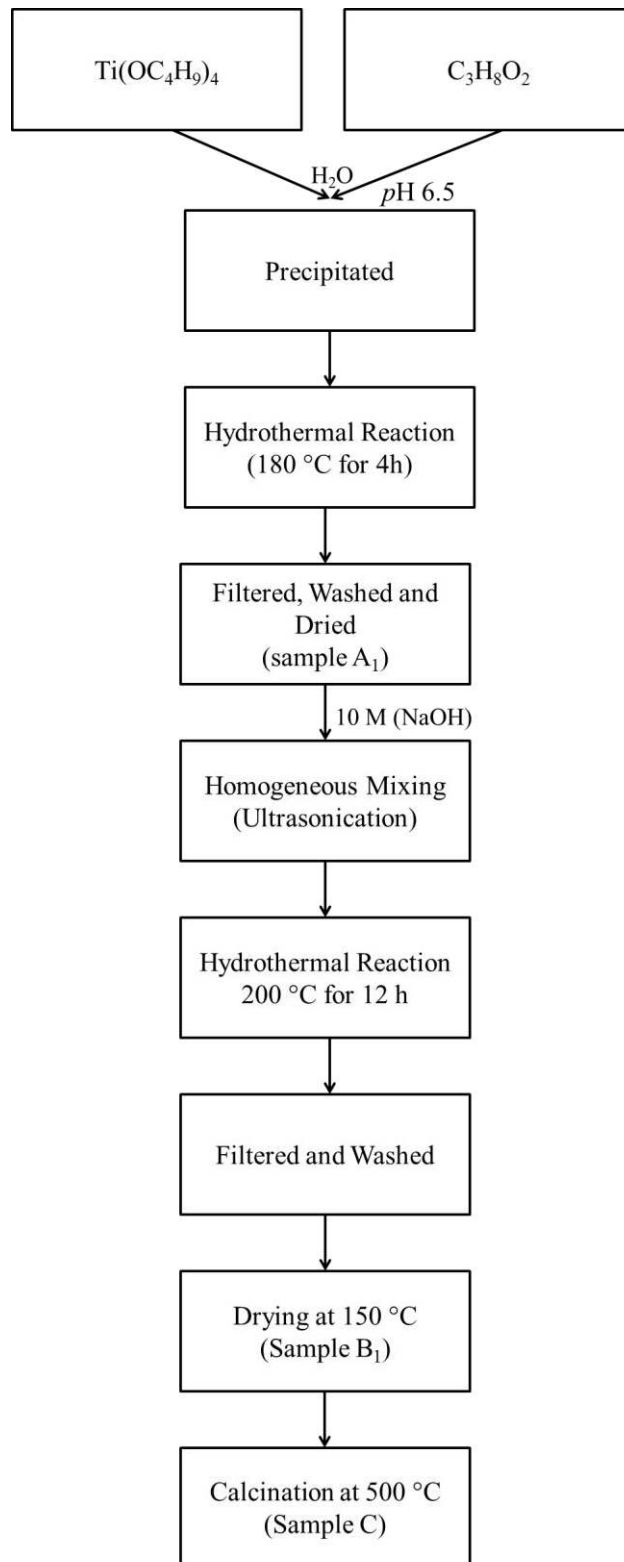


**Fig.3.4** Experimental scheme for synthesis of TiO<sub>2</sub> nanowires using hydrothermal technique.

### 3.1.3 Deposition of Thin Films by Pulsed Laser Deposition Technique

Pulsed laser deposition (PLD) is a versatile technique for deposition of thin films. The main advantages of PLD technique are its flexibility, fast response, energetic evaporants, and congruent evaporation. The deposition unit consists of a target and substrate holder housed in a vacuum chamber. A high power laser is used as an external energy source to vapourise the materials for deposition purpose. A set of optical components is used to focus the laser beam on the target surface. Film growth can be possible in reactive environment containing any reactive gas. The schematic diagram of a PLD system is shown as Fig.3.5. The interaction of laser beam with target material is a complex phenomenon. The mechanism that leads to material ablation depends on laser characteristics, as well as the optical, topological and thermo-dynamical properties of the target. When the laser radiation is absorbed by a solid surface, electromagnetic energy is first converted into electronic excitation and then into thermal, chemical and even mechanical energy to cause evaporation, ablation, excitation, plasma formation and exfoliation.

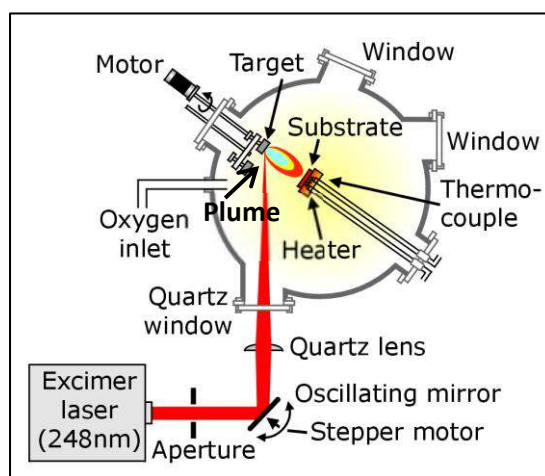


**Fig.3.5** Schematic representation of PLD system depicting various parts.

[[http://www2.physics.colostate.edu/groups/PattonGroup/systems/pld\\_desc.html](http://www2.physics.colostate.edu/groups/PattonGroup/systems/pld_desc.html) on 01 May 2014]

Evaporants form a “plume” consisting of mixture of energetic species including atoms, molecules, electrons, ions, clusters, micron-sized solid

particulates, and molten globules. The collisional mean free path inside the dense plume is very short. As a result, immediately after the laser irradiation, the plume rapidly expands into the vacuum from the target surface to form a nozzle jet with thermodynamic flow characteristics. This process attributes many disadvantages like micron sized particulate formation and the narrow forward angular distribution that makes large area deposition a tedious task [Hubler (1992)].

For the deposition of  $\text{Ti}_{1-x}\text{Co}_x\text{O}_{2-\delta}$  films, the PLD (Lambda PhysikCOMPex 201 Model, Germany) system housed at UGC-DAE CSR, Indore was used. It was using KrF excimer laser ( $\lambda = 248$  nm, pulse width = 20 ns). Films were deposited on commercial Si (p-type, <100> oriented) and  $\text{LaAlO}_3$  (c-axis oriented) substrates. Powders of  $\text{Ti}_{1-x}\text{Co}_x\text{O}_2$  were prepared by sol-gel technique using titanium butoxide and cobalt acetate of analytical grade. Respective targets were prepared by pressing powder samples and were sintered at 900 °C for 12h to achieve high density of the pellet. The diameter of the pellets was around one inch. The target was mounted on the sample holder using silver paste. The Si and  $\text{LaAlO}_3$  substrates were cleaned ultrasonically using trichloroethylene (TCE), acetone, methanol and distilled water subsequently. The targets were ablated at constant laser energy of 240 mJ and 10 Hz repetition rate. A distance of 5 cm was maintained between the target and the substrate. The substrate temperature was maintained at 700 °C during deposition. The base vacuum of the chamber was  $\sim 10^{-5}$  Torr prior to the deposition. Sample deposited at vacuum on Si substrate was maintained at  $10^{-4}$  Torr. Other films were deposited at 0.1 mTorr, 1 mTorr and 300 mTorr oxygen partial pressures on same substrate. For films deposited at 300 mTorr, after deposition, the chamber was filled with ambient oxygen, whereas for other lower oxygen partial pressure, cooling was accompanied with the same deposition oxygen partial pressure. A photograph of the PLD chamber during deposition is shown in Fig.3.6. Similarly, three films were deposited on  $\text{LaAlO}_3$  substrate at 0.1, 10 and 300 mTorr oxygen partial pressure.

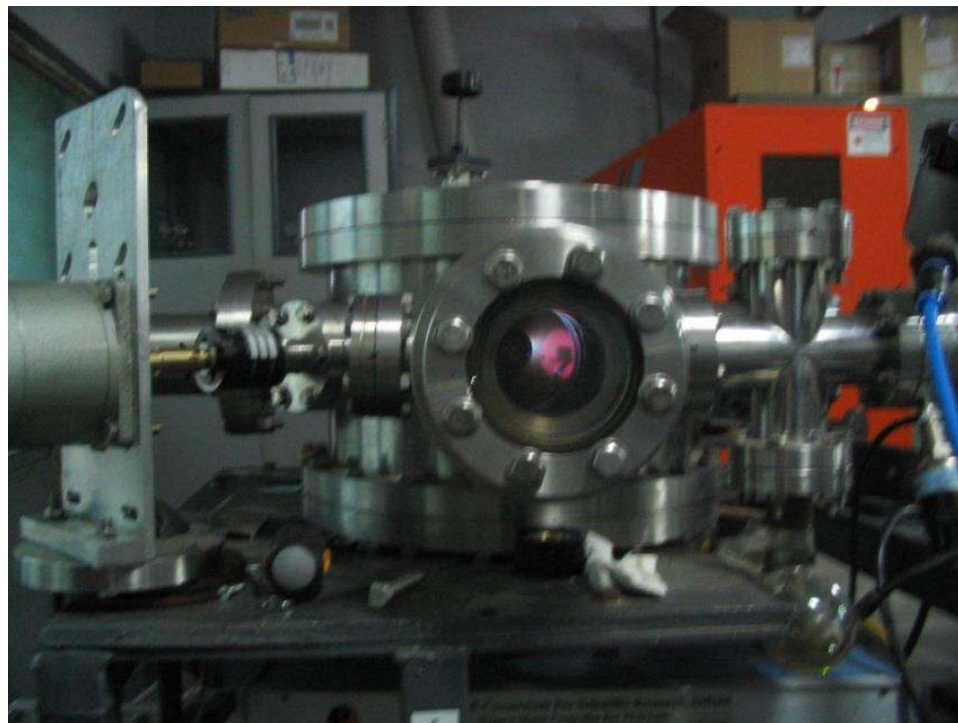


**Fig.3.6** Photograph of the PLD chamber during deposition of thin films.

### **3.1.4 Deposition of Thin Films by e-Beam Evaporation Technique**

In this method, a stream of electron beam is bombarded onto the evaporant material kept in a vacuum environment, so that it attains the vapor pressure necessary for its evaporation. The evaporated material is then allowed to condense on a substrate kept at a suitable distance. The stream of electrons are accelerated through a potential difference of 5-10 kV and magnetically focused onto the surface of the material to be evaporated. The electrons lose their energy very rapidly on striking the surface, and the material, melts at the surface and evaporates. The material is kept in a water-cooled support crucible inside the chamber and the portion in immediate contact with the crucible remains solid. Effectively, the molten material is contained in a crucible of itself and the reaction with the crucible walls is minimized that yields highly pure films [Smith (1995)]. The e-beam evaporation system used for the deposition of  $\text{TiO}_2$  films is shown in Fig.3.7 which is housed at IUAC, New Delhi. The various parts of the deposition chamber are sketched schematically in Fig.3.8.



**Fig.3.7** Electron beam evaporation unit used for the deposition of  $\text{TiO}_2$  film.

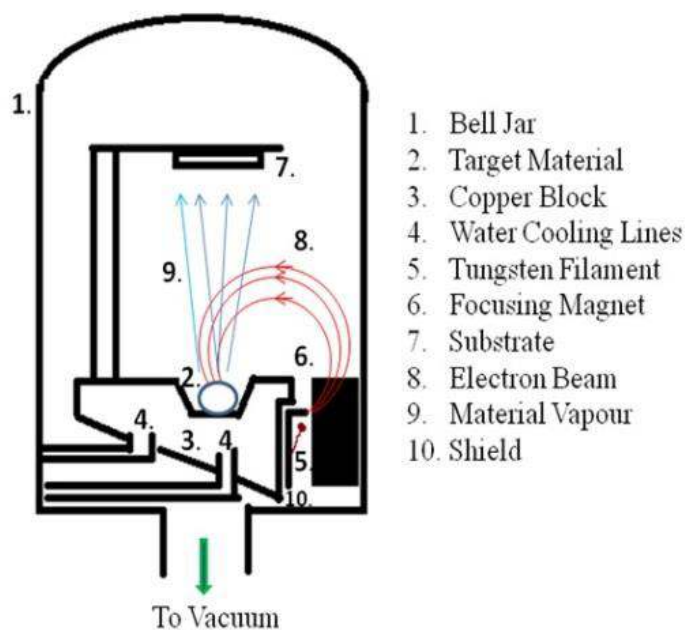


**Fig.3.8** Schematic representation of e-beam evaporation system depicting various parts.



Measurement of the film thickness was carried out by using a quartz crystal thickness monitor placed inside the chamber (not shown in figure). The source to substrate as well as quartz crystal thickness monitor was kept 14 cm. After cleaning the Si (n-type <100>) and Quartz substrates, they were mounted on a sample holder over the source. Liquid nitrogen was used to pour inside the diffusion pump to increase the vacuum level upto  $\sim 1.1 \times 10^{-6}$  mbar before deposition. During deposition, the pressure was maintained at  $\sim 4 \times 10^{-5}$  mbr. Current supplied to the electron gun was kept at 20 mA. The deposition rate was controlled to be 0.2 (1) nm/s. For deposition, high purity TiO<sub>2</sub> target (99.99% from STREM Chemicals, USA) and a piece from the Co-doped TiO<sub>2</sub> target (Co 2 at.%, which was prepared for PLD) was used.

## **3.2 Ion Irradiation Technique**

### **3.2.1 Construction and Working of 15 UD Pelletron Accelerator**

Pelletron at Inter University Accelerator Centre (IUAC), New Delhi, India is a 15 UD tandem Van de Graff type accelerator which can accelerate particles from few tens of MeV to hundreds of MeV. The terminal potential can go upto a maximum of 15 MeV and can produce dc as well as pulsed beam of variety of elements. A schematic diagram of the pelletron accelerator is given in Fig.3.9. The terminal potential is insulated from the ground using SF<sub>6</sub> gas in the tank maintained at a pressure of  $\sim 6 - 7$  atmosphere. The accelerator tank height is 26.5 m with a diameter of 5.5 m. The ion source (Source of Negative Ions by Cesium Sputtering (SNICS)) provides some incident energy to the ions equal to its deck potential. The SNICS source at IUAC can produce a deck potential upto 300 kV. As the ions from the SNICS carry single negative charge, the energy of the ions after leaving the ions source is  $V_d$ , where  $V_d$  is the deck potential. The ions which have trajectory in a horizontal plane are injected into the tank using the injector magnet. This magnet also selects the mass of the ion to be finally accelerated. The terminal of the pelletron, at a positive potential of  $V_T$ , pulls the negative ions imparting them energy of  $V_T$  as they reach the terminal. At the terminal, the ions are passed through a stripper

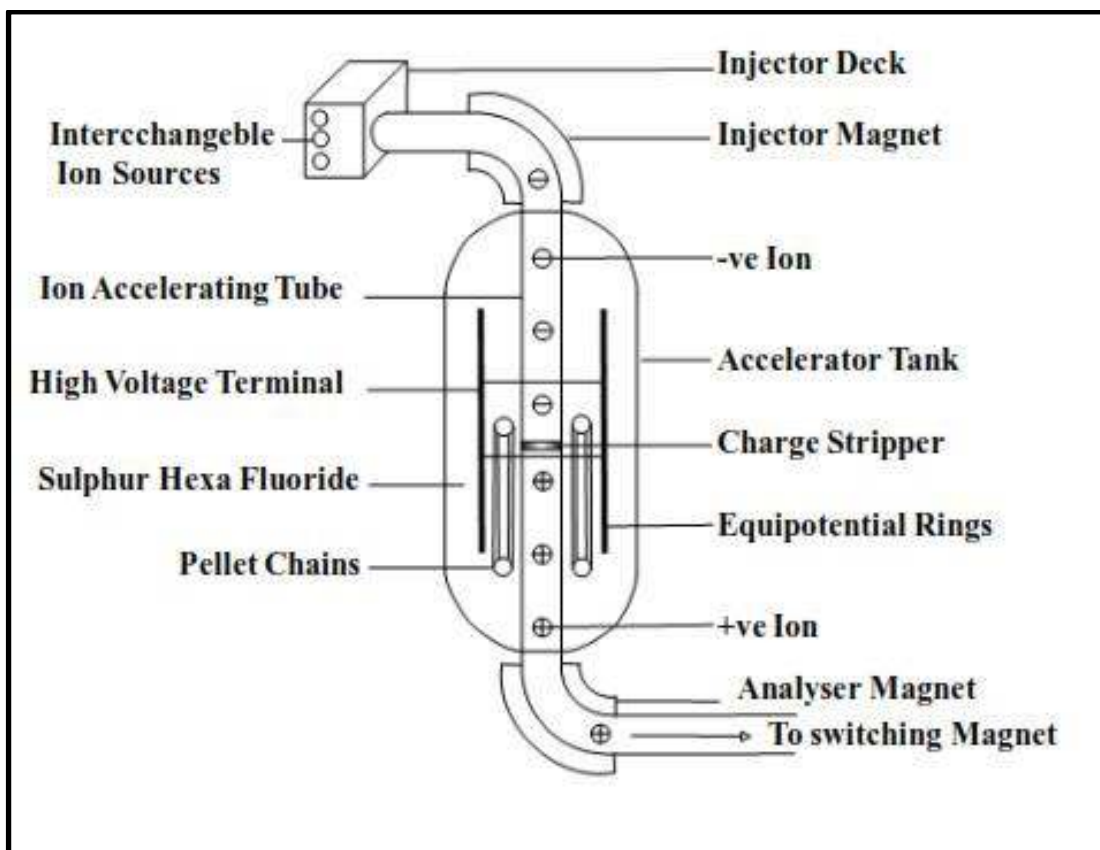


**Fig.3.9** A schematic diagram showing various parts of the Pelletron Accelerator.

foil. The ions lose most of its electrons and become positively charged with some distribution in their charge state.

Ions with various charge states will be present after passing through the stripper foil. If 'q' is the charge on the ion then the total energy gained by the ion through the pelletron will be  $[V_d + (q+1) V_T]$ . The accelerated beam contains ions with various energies and charge states. To select the final energy, analyser magnet is used to pick particular charge state for the given mass of the ions. Apart from selecting particular charge state, analyser magnet also bends the electron beam further to the horizontal plane. The beam from the analyser magnet is then switched (using switcher magnet) to the beam line where the experiment is to be performed. All the operations for tuning the beam for experiments are done from the Control Room.

### 3.2.2 Materials Science Beam Line at IUAC

The Materials Science beam line is at  $+15^\circ$  angle with respect to the direction of the unswitched direct beam. The beam line is maintained at  $\sim 1 \times 10^{-9}$  Torr pressure with the help of ion and getter pumps. The chamber is of 68 cm in diameter and made up of stainless steel. The chamber is pumped by a diffusion pump to attain a pressure around  $2 \times 10^{-6}$  Torr. The chamber is equipped with a light source, camera, a suppressor and setup for ladder current measurement. Suppressor is a hollow metallic cylinder with arrangement for allowing the passage of ions through it. It surrounds the irradiation area with a negative bias (usually 120 V) to suppress the current contribution of secondary electrons emitted from the ladder during the experiment. The target ladder is inserted in the chamber from the top and its vertical motion is controlled by a stepper motor and can be remotely operated from the Control Room. The beam is focused on the target with the help of a magnetic quadrupole and a steerer. For irradiation purpose, the beam is scanned in XY direction over 1 cm x 1cm area with the help of magnetic scanner. The beam can be monitored through the ionoluminescence produced from the quartz crystal attached on the top of the ladder.

We irradiated  $\text{Ti}_{1-x}\text{Co}_x\text{O}_{2-\delta}$  thin films deposited on Si and  $\text{LaAlO}_3$  substrate grown by PLD at different oxygen partial pressures with 100 MeV  $\text{Ag}^{7+}$  ions. The films were pasted on the ladder along its length vertically using double sided tape. The ion fluences were  $5 \times 10^{10}$ ,  $5 \times 10^{11}$ , and  $1 \times 10^{12}$  ions/cm<sup>2</sup> for  $\text{Ti}_{1-x}\text{Co}_x\text{O}_{2-\delta}$  thin films on Si substrate. For  $\text{Ti}_{1-x}\text{Co}_x\text{O}_{2-\delta}$  films on  $\text{LaAlO}_3$  substrate, the fluences were  $1 \times 10^{11}$ ,  $1 \times 10^{12}$ , and  $1 \times 10^{13}$  ions/cm<sup>2</sup>.

## 3.3 Characterisation Techniques

### 3.3.1 X-Ray Diffraction

XRD is a powerful technique to explore the crystal structure and purity of a material. It also gives information regarding the particle size, orientation of crystallites, strain etc. When a beam of x-rays fall on a crystalline material of

particular structure, it is diffracted in different directions. By measuring the angles and intensities of the diffracted beam one can determine the crystal structure. For a particular inter-planer spacing of 'd', the condition for diffraction to occur is given by Bragg's law:  $2d \sin\theta = n\lambda$ . Where 'θ' is the angle between the incident x-ray beam and the sample surface, 'λ' is the wavelength of the incident radiation and "n" is an integer known as the order of the diffraction [Cullity (1978)]. In case of thin films where the thickness is quite small and the intensity of the substrate is dominant, XRD in glancing angle mode is preferable. In glancing angle mode, x-rays are incident on the film surface through a very small angle ( $< 1^\circ$ ) such that the path for the x-rays will increase, and it becomes diffracted without penetrating the film surface.

In this work, an 18 kW rotating anode ( $\text{CuK}_\alpha$ ) based Rigaku (RINT 2000/ PC series) powder diffractometer operating in the Bragg-Brentano geometry and fitted with a graphite monochromator in the diffracted beam was used to record the diffraction patterns for the powder samples. During the XRD measurements of the powder samples, the current was 100 mA and the voltage was 40 kV with  $2\theta$  ranging from 20 to  $80^\circ$ . Le Bail fittings of the XRD profiles were performed using FullProf software package [Rodriguez-Carvajal (1990)]. The Reitveld refinement of the  $\text{TiO}_2$  nanoparticles and nanowires were carried out using JANA software package [Petříček et al. (2006)]. For thin films, Bruker D8 Advance x-ray diffractometer was used accompanied with a fast counting detector based on Silicon strip technology (Bruker LynxEye detector). During the XRD measurements of the thin films, the current was kept 40 mA and voltage was 40 kV. The glancing angle was maintained at  $0.5^\circ$  with  $2\theta$  range from 20 to  $50^\circ$ .

### **3.3.2 X-ray Photoemission Spectroscopy (XPS)**

X-ray photoemission spectroscopy (XPS) or electron spectroscopy for chemical analysis (ESCA) is a surface sensitive technique that provides information about the chemical composition (atomic percent of elements present in the sample), oxidation state (chemical state) of the constituent

elements and valence band structure (density of occupied electronic states). XPS is based on the principle of photoelectric effect. When the sample is exposed to mono energetic x-ray photons of energy  $h\nu$ , it emits electrons from the sample surface. The emitted electrons have kinetic energy (K.E.) given by

$$\text{K.E.} = h\nu - \text{B.E.} - \Phi \dots \dots \dots (5.1)$$

Where ' $h\nu$ ' is the energy of the incident photon, 'B.E.' is the binding energy of the electron and ' $\Phi$ ' is the work function. From the equation 5.1, it is clear that photoelectrons can be produced only if  $h\nu \geq \text{B.E.} + \Phi$  [Stickle (1992)]. The emitted electrons are sorted by their K.E. and the spectrum obtained is a plot of number of emitted electrons per energy interval versus their K.E., known as energy distribution curve (EDC). Since the energy  $h\nu$  of the exciting photons is kept fixed, the B.E. of the electronic states relative to Fermi energy ( $E_F$ ) level can be determined by measuring the K.E. distribution of the photoelectrons. Therefore, the energy distribution of the photoelectrons corresponds approximately to the energy distribution of electronic states in the solid. The photoexcited electrons may scatter with other electrons, plasmons, phonons, and consequently lose part of their energy so that it may not have enough energy to be able to escape at all and change their momentum. One of the consequences of such scattering is the secondary inelastic background intensity, which becomes dominant at the low K.E., principally due to the electron-electron scattering. Since on an average, a photoelectron can travel over a mean free path before being scattered, the electron from a depth of few Å only can reach the detector, making it a surface sensitive technique in spite of large penetration power of x-rays. Finally, the escape from the solid is possible only for those electrons with a K.E. component normal to the surface that is sufficient to surmount the potential barrier offered by its work function. For photoelectron spectroscopy, three main components are required: (i) a photon source, (ii) an energy analyzer for photoelectrons, and (iii) an electron detector. High vacuum is required to increase the mean free path of the electrons coming out of the sample surface and reaching the detector, and to

reduce the contamination layer covering over the sample surface during measurement. Since the photoelectron energy depends on the source energy, the excitation source must be monochromatic. The energy of the photoelectrons is analysed by an electrostatic analyser.

In the present study, we employed XPS instruments from VSW and AMICUS using Al-K $_{\alpha}$  (1486.6 eV) and Mg-K $_{\alpha}$  (1253.6 eV) radiations, respectively. The vacuum level of the sample preparation chamber (SPC) was  $\sim 10^{-8}$  Torr and the sample analysis chamber (SAC) was  $\sim 10^{-9}$  Torr. First, we scanned over the full energy range (survey scan), and then specifically selected O 1s, Ti 2p and Co 2p core level spectra for our study. All observed peaks were calibrated to C 1s peak at 284.8 eV. XPS data were fitted using XPS peak 4.2 software package. For XPS depth profiling experiments 2 keV Ar $^{+}$  ion was used for 40 and 80 minutes, available with the instrument.

### **3.3.3 Raman Spectroscopy**

Raman spectroscopy is a technique based on inelastic scattering of monochromatic light, usually from a laser source. Inelastic scattering means that the frequency of photons in monochromatic light changes upon interaction with a sample. Photons of the laser light are absorbed by the sample and then re-emitted. Frequency of the re-emitted photons is shifted up or down in comparison with original monochromatic frequency which is popularly known as Raman effect. This shift provides information about vibrational, rotational and other low frequency transitions in molecules or solids [Colthup (1990)].

Raman Spectrometers from JobinYvon Horiba (HR 800) and RENISHAW inVia using argon laser source ( $\lambda \sim 488$  nm) were used for the current work. A Si wafer was used as a reference to calibrate the instrument before measurement of desired samples. Raman spectra were recorded in the range of 100 to 800  $\text{cm}^{-1}$  for powder samples, 100 to 1100  $\text{cm}^{-1}$  for Ti $_{1-x}$ Co $_x$ O $_2$  thin films on Si substrate, and 100 to 700  $\text{cm}^{-1}$  for Ti $_{1-x}$ Co $_x$ O $_2$  films deposited on LaAlO $_3$  substrates.

### 3.3.4 Rutherford's Backscattering Spectrometry (RBS)

The knowledge of the slowing down of ions in traversing matter bears fundamental importance in ion beam based characterisation techniques. Depth perception follows directly from the energy lost by the probing particles and the energy loss affects both quantitative and compositional analysis. The physics of energy loss process is a complex interaction between the ion, target nuclei, and the target electrons. In backscattering spectrometry, using ion beams with energies in the MeV range has been used extensively for accurate determination of stoichiometry, elemental density, and impurity distributions in thin films. Ions to be analyzed scatter elastically from target atoms with energy characteristic of the mass of the struck particle. They also lose energy during passing into and out of the film material. Energy analysis of the backscattered ions by the detection system yields the backscattering spectrum in the form of counts per channel vs. channel number. The channel number is linearly related to the backscattered energy. A nearly flat topped 'peak' is appeared for each element present in the film. The peak widths are caused by the energy loss of the analysis ions in the film material [Chu (2012)].

A Pelletron Accelerator (1.7 Million Volt) based RBS system installed at IUAC, New Delhi was used to characterise the thin films. It was equipped with: (i) Alphatross ion source for producing negatively charged He and H ions, (ii) 1.7MV 5SDH-2 Pelletron accelerator and (iii) Charles Evans and Associate make 4 - axis goniometer (model name RBS-400). Surface barrier detector was used to measure the number and energy of ions backscattered after colliding with atoms of the sample enabling us to determine atomic mass and elemental concentration versus depth below the surface. Thin films of  $Ti_{1-x}Co_xO_2$  deposited on Si,  $LaAlO_3$  and a piece of target material were mounted on the sample holder using carbon tape. For calibration of the instrument, a gold film deposited on glass substrate was used. Sample positions were varied automatically using a goniometer controlled by a computer. The RBS spectrum of a typical Co-doped  $TiO_2$  target is shown in Fig.3.10. Simulation was done

using the RUMP software package. Black line represents the experimental data and the simulated spectrum is shown in red. The average Co concentration in the target was found to be two atomic percent. No other elements besides Ti, Co and O are observed.

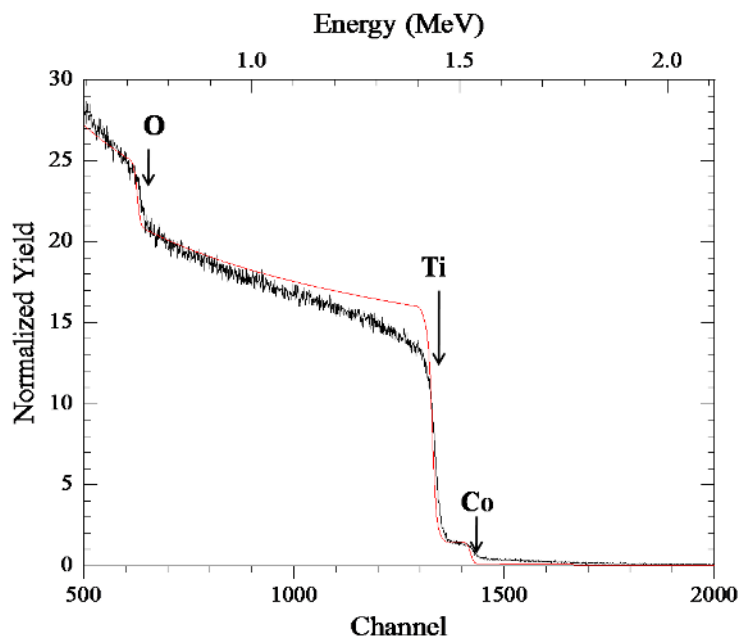


**Fig.3.10** RBS spectra of CTO target (black line is the experimental data and the simulated spectrum is shown in red)

### 3.3.5 Transmission Electron Microscopy (TEM)

Transmission electron microscopy (TEM) uses high energy electrons to penetrate through a thin ( $\leq 100$  nm) sample. This offers increased spatial resolution in imaging (down to atomic scales) as well as the possibility of carrying out diffraction from nano-sized volumes. When electrons are accelerated upto high energy levels (few hundreds keV) and focused on a material, they can scatter or backscatter elastically or inelastically, or produce many interactions, source of different signals such as x-rays, Auger electrons or light [Willams and Carter (1996)]. To find out the size, shape of nanoparticles and aspect ratio of nanowires, we used a TEM from Tecnai G<sup>2</sup>T 30. The same system was used to view the cross-section of the undoped and Co-doped TiO<sub>2</sub> film deposited on Si substrate. Sample preparation method is given as:



**(i) For powder samples:**

Few milligram of powder samples were dispersed in 50 ml of ethanol and ultrasonicated for homogeneous mixing. Then a drop from the solution was casted on the commercial TEM grid (carbon coated copper grid). Further, the grid was dried to evaporate the volatile alcohol. Similar method was adopted for investigating TiO<sub>2</sub> nanowire samples.

**(ii) For Thin Films:**

To make solid sample for cross-sectional TEM, an 1cm x 1cm film was cut from the middle and glued between its two surfaces. Then few Si substrates were pasted from the back side of the substrate to increase the thickness. After that a cylindrical portion of the stacked film was drilled along its cross-section and inserted into a hollow Cu tube in such a way that the cross-section of the sandwich will positioned at the middle of the tube. Then the tube was cut into slices with the help of a diamond cutter. Then the above slice was thinned mechanically by polishing, dimple grinding and finally by Ar ion milling. For the present study, we selected two films for cross-sectional TEM, one is Ti<sub>1-x</sub>Co<sub>x</sub>O<sub>2-δ</sub> film deposited on Si substrate at 300 mTorr oxygen partial pressure by PLD technique. Another is a TiO<sub>2</sub> film deposited on Si substrate by e-beam evaporation technique and annealed at 500 °C under oxygen flow for 1h.

**3.3.6 Scanning Electron Microscopy (SEM)**

It is an important non-destructive tool to analyse the magnified images of metallic, semiconducting and insulating materials. It uses accelerated electrons instead of visible light to form an image. A stream of electrons is produced by an electron gun and is accelerated from few hundred eV to 40 keV. The electron beam follows a vertical path through the microscope, which is held in within a high vacuum. The beam is focused using magnetic lenses to a spot size of about 0.4 to 5 nm in diameter on the sample surface. Once the beam hits the sample, electrons and x-rays are ejected from it. Detectors collect these x-rays, backscattered electrons, secondary electrons and convert them

into a signal that can be visualized on a computer screen. The electron beam is scanned, or ‘rastered’ across the sample via magnetic scan coils. The current produced due to the backscattered electrons is collected, amplified and plotted as a two-dimensional image or ‘micrograph’ of the signal intensity. For SEM, samples should be conducting to ensure no charging during the measurement.

For the present study, a field emission gun based scanning electron microscope (FE-SEM) (Supra 40, Zeiss, Germany), equipped with energy dispersive x-ray analyzer was used. TiO<sub>2</sub> nanowires, films and Co-doped TiO<sub>2</sub> films were mounted on the sample holder using carbon tape. TiO<sub>2</sub> nanowires were coated with conducting gold layer by sputtering, under vacuum before recording the images to avoid charging. The gun voltage was varied to capture well focused image of the sample. Compositional analysis was carried out by the energy dispersive x-ray spectroscopy (EDS) available with the above system. Its working principle is that each element has a unique atomic structure allowing emission of x-rays that are characteristic of that particular element which is distinguishable from the x-rays emitted by another element.

### **3.3.7 Scanning Probe Microscopy (SPM)**

Scanning probe microscopy (SPM) comprises a group of techniques that measure surface topography and their properties. Among them we used AFM (Atomic Force Microscopy) and MFM (Magnetic Force Microscopy) to characterise the thin films. An AFM consists of a cantilever with pointed piezoelectric tip at the end which is used to scan over the sample surface. When the tip approaches the sample surface, forces between the tip and the sample lead to a deflection of the cantilever. The deflection produced is measured using a laser spot reflected from the cantilever surface into an array of photodiodes. The photodetector converts the difference in laser signals into voltage that reconstructs the surface topography. Feedback from the computer maintains the tip either at a constant force or constant height above the sample surface. MFM’s working principle is similar to AFM, where a sharp magnetised tip scans over the magnetic sample. The magnetic interactions

between the tip and sample are detected and reconstructed on a computer screen. The ferromagnetic or antiferromagnetic interactions between the tip and the sample gives rise to colour contrast in the MFM images [Rugar et al. (1990)]. MFM is quite sensitive and able to capture the domain walls in magnetic specimens.

AFM was done using a Scanning Probe Microscope (SPM) from Veeco Instruments. Imaging was done in SPM mode with the help of Berkovich tip from Hysitron. Software employed for analyzing SPM image was NanoScopeIV (version 5.30r1, 2004) controller supplied by Veeco Instruments. MFM measurements were carried out using a Scanning Probe Microscope from Digital Instruments Nanoscope installed at UGC-DAE CSR, Indore.

### **3.3.8 UV-visible Spectroscopy**

A spectrometer is an optical device that transmits a specific band of electromagnetic spectrum properly selected with the help of refraction (through prism) or by diffraction (diffraction grating). It helps in determination of absorbance of the material or analysis of the emission from the excited atoms or molecules. Materials with known absorbance or band gap can easily be identified with the UV-visible spectroscopy.

For the experiments, we used double beam spectrophotometers to record the absorbance of the samples (Shimadzu (Model 2450) and Hitachi U 2900). In a double beam spectrophotometer, one beam is incident on the sample and other one on the standard reference ( $\text{BaSO}_4$  powder). A photomultiplier tube (PMT) was used to record the spectra. The light source used for UV was a hydrogen or deuterium lamp and for visible range a tungsten lamp was used. For powder samples, measurements were carried out in the diffused reflectance mode using an integrating sphere assembly provided with the Shimadzu 2450 spectrophotometer. Reflectance was converted to absorbance using the Kubelka-Munk function. Thin films of  $\text{TiO}_2$  deposited on quartz substrate and annealed under oxygen and argon flow at 500 °C for 1h using e-beam

evaporation technique were used for the UV-visible study using Hitachi U 2900 double beam spectrophotometer.

### **3.3.9 FT-IR Spectroscopy**

In FT-IR spectroscopy, infrared radiation is passed through the sample. Some of the radiation is absorbed by the sample and rest is transmitted. An infrared spectrum represents a fingerprint of a sample with absorption peaks which corresponds to the frequencies of vibrations between the bonds of the atoms constituting the material. Because each different material is a unique combination of atoms, no two compounds produce the same infrared spectrum. Therefore, infrared spectroscopy is useful for identification (qualitative analysis) of different kinds of material. In addition, the size of the peaks in the spectrum is a direct indication of the amount of material present. With modern software algorithms, infrared is an excellent tool for quantitative analysis. FT-IR is useful in identifying unknown materials with determination of functional groups present in the material.

In the present work, FTIR spectrometer from Bruker, Germany, Model: Vertex 70 was used. Standard KBr technique was followed for the sample preparation.

### **3.3.10 Magnetic Measurements**

Magnetic measurements reveal the magnetic state of a material. The basic measurements include the measurement of magnetization as a function of temperature with a constant probing field. Magnetization as a function of applied external magnetic field at constant temperature also helps to get the magnetic behaviour of the material. In this work, we used a commercial VSM (PPMS from Quantum Design, USA), a superconducting quantum interference device (SQUID: MPMS XL from Quantum Design, USA) and superconducting quantum interference device - vibrating sample magnetometer (SQUID-VSM from Quantum Design, USA). The facilities were utilized at UGC-DAE CSR,

Indore, India. Brief descriptions of the working principle of each are given below.

### **Vibrating Sample Magnetometer (VSM)**

DC magnetization measurements of undoped and Co-doped TiO<sub>2</sub> nanoparticles were carried out using a commercial VSM having specification with temperature ranging from 2 - 400 K and field  $\pm 14$  Tesla. For the measurement of magnetic moment, a VSM involves induction method that refers to the measurement of voltage induced in a set of detection coils by a varying magnetic moment. In this process, sample under investigation is made to vibrate in a uniform magnetic field that induces voltage at the detection coil. For instance, if a magnetic dipole, initially placed in the center of a pickup (detection) coil, is moved to a distance then a flux ( $\phi$ ) is produced that results in inducing a voltage ( $v = d\phi/dt$ ) in the detection coil. The pickup coils may be located inside a solenoid (for generating magnetic field), so that the moment can be measured as a function of the externally applied magnetic field [Foner (1959)].

### **SQUID Magnetometer**

SQUID is the most sensitive instrument available to measure the magnetic field. However, it does not detect the magnetic field from the sample directly. The sample is made to move through superconducting detection coils, which are coupled to the SQUID through superconducting wires, allowing the current from the detection coils to inductively couple to the SQUID sensor. The basic function of a SQUID is to convert current to voltage sensibly. The instrument essentially contains the following parts: the SQUID (main unit of the device), a magnetic flux transformer including pickup coils, the superconducting magnetic coil, heat switches and magnetic shielding. Superconducting detection coils are configured as a second-order gradiometer, with counter wound outer loops that make the set of coils non-responsive to uniform magnetic fields and linear magnetic field gradients. The detection coils

only generate a current in response to local magnetic field disturbances [Clarke (1996)]. The superconducting magnetic coils are used to apply large magnetic fields. Since SQUID is extremely sensitive to minute fluctuations of the magnetic field, magnetic shielding is inevitable to shield the sensor itself both from the fluctuations in the ambient magnetic field of the laboratory as well as from the large magnetic fields produced by the superconducting coil. Heaters are used to heat up a small section of the detection coil circuit whenever the magnetic field is changed. They allow the elimination of standing currents in the superconducting loops by raising them beyond their critical temperature.

### **SQUID –Vibrating Sample Magnetometer (SQUID-VSM)**

It is a modified version of SQUID magnetometer. It records the magnetic moment of the sample combining the sensitivity of a SQUID and speed of a VSM. The sample is vibrated at a known frequency and phase-sensitive detection is employed for rapid data collection and spurious signal rejection. It is worth noting here that the sample vibration is anyhow not the essential requirement to produce the signal as in a conventional copper-detection-coil VSM where a changing magnetic flux is a must. Instead, the sample vibration is used only to create a signal at a known modulation frequency to aid the separation of the sample signals from the instrumental artifacts. The size of the signal does not depend on the vibration frequency and higher vibration frequencies will not improve the signal to noise ratio, as in a conventional VSM. This is due to the use of superconducting detection coils that produce a current in response to magnetic flux, instead of causing change in magnetic flux as produced by copper coils.

### **3.3.11 Transport and Magneto-transport Measurements**

The most popular technique for the measurement of resistivity of a material is either two probe or four probe techniques. For high resistance material two probe technique is commonly used. Whereas for metallic, semi-metallic samples: four probe technique gives precise results. In a two probe

method, each probe serves as a current as well as a voltage probe. Basically, a known voltage is applied across the sample and corresponding flow of current is measured. In two probe method, the resistance due to the contacts as well as connecting wires contributes to the net resistance of the material. For high resistance materials, these contact resistance is negligible. But in case of metallic samples these contact resistances contribute significantly so that the exact resistance of the material cannot be determined precisely. However, in a four probe technique, a constant current is passed through the outer two probes and corresponding voltage drop is measured across the inner two probes. The voltmeter draws negligible or no current due to its high internal resistance. So, it measures resistance of the sample only.

We measured resistivity of thin films of size approximately 5 mm x 5 mm by using four probe technique. For the electrical contacts, indium was used (highly conducting and thermally insulating material) and thin copper wires were used for electrical connections for their low resistivity. Fig. 3.11 demonstrates the geometry of the four probe connections. Here 'b' is the length of the film, 't' is the thickness of the film and 'l' is the distance between the voltage probes. The substrate is not shown in the diagram.

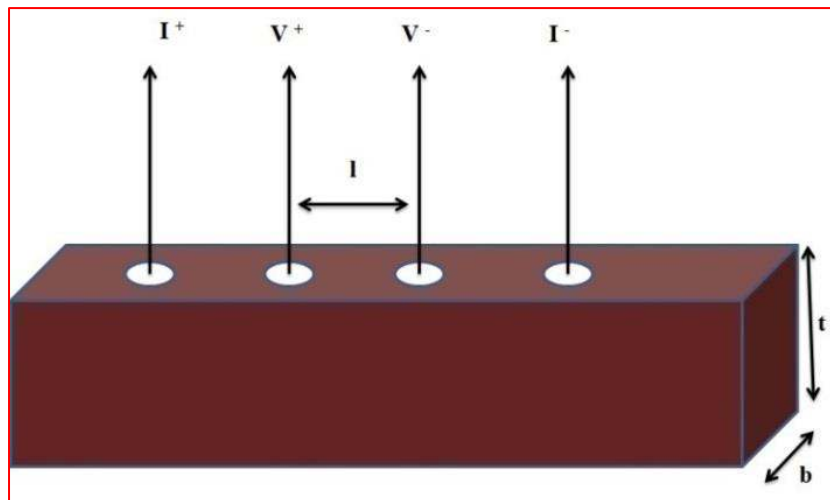


**Fig.3.11** Typical four probe arrangement

Magnetoresistance (MR) is defined as the relative change in materials resistivity on the application of an external magnetic field. Numerically, MR is represented in percentage as given below:

$$\text{MR (\%)} = \frac{\rho_H - \rho_0}{\rho_0} \times 100$$

In the present study, the magneto transport properties were measured with standard four probe method as discussed earlier from 300 K to 5 K using Advantest current source and Keithley nano-voltmeter. Maximum applied dc magnetic field was 8 Tesla using a superconducting magnet system “Spectromag<sup>2000</sup>” supplied from the Oxford Instruments. Current was parallel to the applied magnetic field direction (with maximum resistance 1 mega ohm).